Workability and compressive strength development of self-consolidating concrete incorporating rice husk ash and foundry sand waste – A preliminary experimental study

Sua-iam, Gritsada; Makul, Natt; Cheng, Shanshan; Sokrai, Prakasit

Published in:
Construction and Building Materials

DOI:
10.1016/j.conbuildmat.2019.116813

Publication date:
2019

Workability and compressive strength development of self-consolidating concrete incorporating rice husk ash and foundry sand waste — A preliminary experimental study

Gritsada Sua-iam[a*], Natt Makul[b], Shanshan Cheng[c], Prakasit Sokrai[a]

[a] Department of Civil Engineering, Faculty of Engineering at Rajamangala University of Technology Phra Nakhon, 1381 Pibul Songkhram Road, Bangsue, Bangkok 10800

[b] Department of Building Technology, Faculty of Industrial Technology, Phranakhon Rajabhat University, 9 Changwattana Road, Bangkhen Bangkok, 10220, Thailand

[c] School of Engineering, Plymouth University, Drake Circus, Plymouth PL4 8AA, United Kingdom

[*]Corresponding author. Tel. (662) 544-8456 and Fax: (662) 522–6637

E-mail: gritsada.s@rmutp.ac.th (G. Sua-iam).

Abstract

The combined advantages of wastes in high-performance concrete production are currently popular topics of investigation. This study aims to examine the effect of foundry sand waste (FDW) as a fine aggregate replacement (30 and 50%wt) on the properties of self-consolidating concrete (SCC) mixed with untreated rice husk ash (RHA) as a cement replacement (10 and 20%wt) with controlling water-binder materials ratios (w/b) of 0.35 and 0.45. The workability and strength characteristics of SCC are considered. The results indicate that the increase in FDW amount affects the SCC with RHA, increases the required superplasticizer and setting times compared to the control SCC, and decreases the density and slump flow loss. The incorporation of RHA and FDW decreases the filling and passing ability

of the SCC. Based on the workability requirements specified by EFNARC guidelines, SCC mixtures exhibited acceptable V-funnel performance at replacement levels of RHA and FDW not more than 10 and 30 wt% and achieved the highest compressive and splitting strengths.

Keywords: Self-consolidating concrete; Foundry sand waste; Rice husk ash; Workability Compressive strength

1. Introduction

Almost 30 years ago, in 1993, at the University of Tokyo, Japan, self-consolidating concrete (SCC) was proven to have the advanced potential for applications in modern construction [1]. SCC has high-performance characteristics such as high flowing when the fluid fills into complicated moulds and passes congested reinforcing steel without excessive segregation [2], channel, and normal bleedings. SCC can also develop highly early- and long-term mechanical properties and durability [3]. These numerous potentials resulted in the continuously increasing demand for concrete construction materials and related concrete composites in the present [4,5]. However, a small disadvantage of SCC, particularly powder-type SCC, is the requirement for a high powder content to overcome the lubrication and fluid nature of SCC, which causes autogenous shrinkages. Moreover, the high pure-cement content (control SCC) increases the high temperature from hydration and causes thermal cracking in the concrete structure, which affects long-term durability [6,7]. One of these negative effects can be resolved by using pozzolan materials such as fly ash, silica fume, meta-kaolin, etc. In addition to reducing the cement content, pozzolan materials such as rice husk ash (RHA) can improve the early- and later-stage compressive strength and decrease the water permeability of SCC [8].

Currently, RHA is a valued by-product from the burning process of rice husk/hull to produce electricity worldwide [9]. Because RHA has a similar intrinsic heating value to coal, rice-based agricultural countries can produce a reasonable amount of electricity using rice husk/hull; the by-product is RHA with 20–25%wt remnants from burning, which can be used as cement replacement material. Originally, RHA was disposed into landfills and induced high costs of environmental management because of the long-term treatment [10,11]. Thus, the use of RHA as cement replacement materials is a sustainable method but must be investigated for characterization and practical applications.

RHA can be used to produce concrete and affects numerous properties, such as the internal pore structure, setting time, and compressive strength development [4,9]. However, the high porosity of RHA particles requires a high dosage of superplasticizer and makes it harder to mix, compact, and finish the concrete. Therefore, the optimal RHA content to produce high-strength and high-performance concrete is 20%wt [11,12].

Apart from the use of RHA as an OPC replacement material, the effects of fine and coarse aggregates on the properties of SCC should be considered; in particular, in most SCC production, the quality and quantity of fine aggregate are dominant factors to control SCC behaviour. Because of the shortage of fine aggregate, e.g., natural sand, this study examines the possibility of recycling foundry sand waste (FDW) as a fine aggregate (river sand) replacement.

FDW is the main by-product of the casting process in the production of internal and external engine parts [13,14]. Currently, numerous studies are investigating the effect of this waste on concrete properties for use as filler, embankments, etc. [15,16]. FDW has been suggested as a fine aggregate replacement [17-21]. For example, Pathak and Siddique [3] used spent foundry sand at 10%wt replacement in sand and heated the concrete specimen at a high temperature. The results show that there is a little enhancement in compressive strength, but the

viscosity-modifying admixture dosage decreases. However, most studies focused on this point and no study examined the use of FDW in SCC production.

With highly porous RHA particles, RHA-mixed SCC exhibits limitations in practical production and usage. The FDW incorporation may affect the properties of SCC in both fresh and hardened states, which has not been thoroughly investigated and will be the novelty of this study. Combining the advantages of the materials is significant for improving the SCC and elimination of waste, which is a selection point for environmentally friendly SCC and the combined benefit of these materials. Due to the valuable combined advantages of the materials, the objective of this study is to incorporate the use of untreated RHA as the cement replacement material and of FDW as the fine aggregate replacement in the SCC production. As mentioned, RHA is used in ordinary Portland cement (OPC) at limited contents of 20%wt and FDW is used to fill the voids within RHA particles.

2. Materials and methods

To achieve the objective of this study, specific mixtures of RHA and FDW were developed. First, the water-binder materials (OPC and/or RHA) with w/b ratios of 0.35 and 0.45 were controlled while maintaining the binder materials of 650 kg/m^3. The RHA replacement in the OPC content was 10 and 20%wt, whereas the FDW replacement of fine aggregate (river sand) was 30 and 50%wt. In total, 14 SCC mixtures were designed and experimentally investigated as shown in Table 1. The standard OPC was produced in Thailand with a specific gravity of 3.14 ± 0.02. Its properties were in accordance with ASTM C150/C150M−12 [22]. Here, the properties of the control SCC and RHA-containing SCC were compared. The local coarse aggregate was crushed limestone rock, whose gradation complied with ASTM C33/C33M−18 [23]. The properties of river sand were specified in ASTMC33/C33M−18 [23]. The specific gravities of the crushed rock and river sand were 2.64

and 2.72, respectively. The chemical admixture as superplasticizer (Type G) was specified in ASTM C494/C494–17 [24] with a constant dosage of 1,200 cc. / 100 kg of binder materials (OPC and RHA) and had a solid content of 42.5%wt. This admixture was used to control the target slump range at 70.0 ± 2.5 cm. Every SCC specimen was demoulded at 23.5 ± 0.5 hours after mixing and continuously cured in lime-saturated water at a controlled temperature of 25 ± 2 °C until the test time. The test properties are the workability (filling and passing properties), slump flow loss, setting time, and strength characteristics (compressive strength, splitting tensile strengths, and their relationships).

2.1 Materials

The RHA in this study was collected by dust collectors, which were similar in size and working mechanism to a local electric power plant in Thailand. This plant used rice husk as the main fuel to burn boilers at a burning temperature of 870 ± 20 ^{0}C and drive generators to produce electricity. In the SCC mixtures with RHA, RHA was untreated and used as received. RHA had a high SiO_2 content (91.45 ± 1.34% by mass) as detected by X-ray fluorescent (XRF) as shown in Table 2. Moreover, the RHA particle size, represented with a 50% cumulative passing, was 22.31 ± 0.88 μm, larger than the OPC particles 13.50 ± 0.39 μm. The specific surface area was measured using the Brunauer, Emmett and Teller (BET) method; RHA had a smaller specific surface area (364 ± 9.04 m^2/kg) than OPC particles (382 ± 5.02 m^2/kg).

FDW was obtained from the casting process of the production unit of an engine-part factory in Thailand. It was directly used as a fine aggregate (river sand) replacement in 30 and 50 wt% with no improving treatment method. The specific surface area of FDW, which was calculated as mentioned, was 341 ± 8.25 m^2/kg.

As shown in Fig. 1, the percentage cumulative passing distributions of OPC, RHA, and FDW were calculated and analysed using a laser diffraction particle size analyzer. The results

show that the sizes of OPC, RHA, and FDW particles are 0.1–403.2 μm, 0.7–91.1 μm, and 0.2–190.1 μm, respectively. When FDW replaces river sand, it can act as a filler compared to the particle size of river sand. In other words, the smallest size of sand particles from sieving in accordance with ASTM C33/C33M−18 [23] was 1.49×10^{-2} cm, which was rather larger than that of the mixture with 50% cumulative passing of FDW (0.239×10^{-2} cm) (the preliminary sieve analysis of river sand in percentage passing in this study was: 9.51×10^{-1} cm) = 100%, No. 4 (4.76×10^{-1} cm) = 97.3, No. 8 (2.28×10^{-1} cm) = 86.10, No. 16 (1.19×10^{-1} cm) = 66.03, No. 30 (5.95×10^{-2} cm = 31.91), No. 50 (2.97×10^{-2} cm) = 5.66, and No. 100 (1.49×10^{-2} cm) = 0.72).

The morphologies of OPC, RHA, and FDW are shown in Fig. 2. Compared to OPC particles, RHA particles are larger and more porous but have smooth surfaces and slightly irregular shapes. The high porosity of RHA increases the superplasticizer demand to achieve the targeted slump flow. Compared to OPC particles, FDW particles have more irregular shapes, similar to sand particles, and are mostly larger in size. Some larger particles of FDW are accumulations of smaller particles.

2.2 Items of investigation

2.2.1 Fresh-state properties of SCC

To achieve the targeted slump flow in SCC production (the measured slump flow must be at least in the range of 70.0 ± 2.5 cm), the properties of SCC can be mainly classified into filling and passing abilities. The filling ability is the ability to fill the mould under its gravitational weight and can be determined by ASTM C1611/C1611M−14 [25]. The passing ability can be evaluated according to ASTM C1621/C1621M−17 [26]. Moreover, we evaluate the V-funnel flow time [27], unit weight compliance with ASTM C138/C138M−17a [28], and setting time in accordance with ASTM C403/C403M−16, standard [29].

2.2.2 Hardened-state properties of SCC

The methods to test the compressive and splitting tensile strengths of SCC are in accordance with ASTM C39/C39M−18 [30] and ASTM C496/C496M−17 [31], respectively. Three-hundred and seventy-eight-SCC specimens with a diameter of 15.2 cm and height of 30.4 cm were cast and continuously cured until the test time at 3, 7, 14, 28, 56, 90, 120, 150, and 180 days. The strengths were evaluated by averaging three values. Moreover, the relationships of the compressive-splitting tensile strengths were calculated.

3. Results and discussion

3.1 Properties of fresh SCC

3.1.1 Superplasticizer requirement to achieve the targeted flow slump of SCC

To achieve the targeted flow slump of SCC (70.0 ± 2.5 cm), the superplasticizer requirement of each SCC mixture was determined and is presented in Fig. 3. Compared to the control SCC (65R0FDW0), an increase in OPC content increases the water requirement from 0.92 to 1.20% per 100 kg binder materials, which implies that a higher surface area requires more superplasticizer to overcome the internal particle friction and create flowability. This behaviour is similar for RHA-containing SCC at w/b ratios of 0.35 and 0.45 because the high porosity of RHA particles increases the superplasticizer doses. The requirements of 0.35-w/b SCC 65R10FDW0 mixture increased of 1.82%, whereas that of 65R20FDW0 increased of 2.10%. However, when w/b increased from 0.35 to 0.45, the superplasticizer demand of the 65R10FDW0 mix decreased of 0.27%. The mixture of 65R20FDW0 had an identical tendency.

Regarding the effect of FDW in the superplasticizer requirement, it was observed that the FDW replacement increases superplasticizer requirement compared to the control SCC and RHA-mixed SCC. The increase is more significant when the replacing ratio is 50%wt because the SCC mix has more FDW, which are finer particles than sand. Therefore, the SCC mixed

with FDW requires a higher dosage of superplasticizer. The requirement of the SCC mixed with FDW was higher than that with w/b ratios of 0.35 and 0.45 because the increase in amount of finer particles of FDW requires more water.

3.1.2 Fresh density

Table 3 shows the densities of fresh SCC mixed with RHA, or RHA and FDW. The increasing amount of RHA results in a lighter fresh density compared to the control SCC because of the lower specific gravity of RHA compared to cement particles: the densities of 65R10FDW0 and 65R20FDW0 are 0.60 and 1.24% that of SCC, respectively. Moreover, when FDW replaced sand, the 0.35 w/b-SCC was lighter than the control SCC and RHA-mixed SCC, e.g., 65R10FDW30 has a decrease of 1.20%, and 65R10FDW50 has a decrease of 1.60%.

For the SCC containing RHA and FDW, the fresh density decreases with more FDW. Thus, the mixture of FDW and fine (river sand) aggregate has a stronger effect than the sand replacement by FDW and RHA replacement in OPC. For the RHA replacement in OPC, the fresh density is lower than that of the control SCC.

3.1.3 Filling ability

As mentioned, the SCC was set to have a slump flow value of 70.0 ± 2.5 cm. The filling ability can be evaluated using the V-funnel flow time in accordance with EFNARC [27]. As shown in Table 3, the control SCC mixture of 65R0FDW0 took 7 s to decrease their viscosity.

When RHA is included in SCC, the V-funnel flow time increases with more absorption of RHA particles, as shown in Fig. 4. For example, the flow time increased from 7 s to 9 s (65R10FDW0) and 10 s (65R20FDW0). Although there was more RHA, OPC had a higher content to overcome the friction between OPC-OPC, OPC-RHA, and RHA-RHA particles.

199 The replacement addition of FDW significantly affected the flow time. In detail, the
200 RHA-SCC mixture containing FDW increased the flow time by approximately 1.5 times on
201 average, respectively, because the high content of FDW increased the viscosity of SCC
202 compared to the control SCC mixed sand, which makes the SCC mixture form agglomerates
203 and makes it difficult to flow across the small V-shaped opening.
204 Fig. 5 shows the slump flow loss at 120 minutes after mixing the SCC. The slump flow
205 loss of the control 0.35-w/b SCC decreased by 21.4% because of the OPC absorption and
206 increase in hydration reaction. The 0.45-w/b SCC had less slump flow loss than the 0.35-w/b
207 SCC mixtures because of the higher water content in the mix. When RHA was replaced in the
208 OPC, the SCC had lower slump flow loss than the control SCC because of the lower
209 flowability of water absorbed by RHA particles. The SCC mixed with FDW also had a lower
210 slump flow loss than the control SCC and SCC containing RHA. Moreover, the SCC at 0.45-
211 w/b had a lower slump flow loss than the 0.35-w/b SCC because of the high free-water content.
212 Thus, when a high amount of water is absorbed at the saturated point, we can maintain the
213 fresh state of SCC and limit the low reactivity of the OPC's hydration reaction, which reduces
214 the slump flow loss.
215 Based on the workability requirements specified by The European Federation of
216 Specialist Construction Chemicals and Concrete Systems (EFNARC) guidelines for V-funnel
217 flow times to be 8–12 s [27], SCC mixtures exhibited acceptable V-funnel performance when
218 they made RHA and FDW at replacement levels of RHA and FDW not more than 10 and 30
219 wt%.
220
221 **3.1.4 Passing ability**
222 To evaluate the passing ability of SCC, as specified in the ASTM C1621/C1621M–17
223 [26], the results from the J-ring test are shown in Table 3. As expected, the control SCC had no

visible blocking. However, there was no occurrence for the SCC mixture with 10 and 20%wt RHA because of the increasing OPC content, as observed from the remaining amounts of 65R20FDW0 OPC, which was 520 kg/m^3. This result can imply that when using RHA to produce SCC, the OPC content at 520 kg/m^3 or more should be specified.

3.1.5 Setting time

Fig. 6 shows the initial and final setting times of SCC with/without RHA or FDW for (a) 0.35-w/b and (b) 0.45-w/b. For the control SCC (Fig. 6 (a)), the setting times of SCC decreased with increasing OPC content according to the high hydration reaction rate of OPC. Nevertheless, when RHA is used in OPC, the setting times of SCC were extended (increased) due to the low pozzolan reaction of RHA in the early setting stage. The setting times of SCC with FDW also increased because of the low reaction of FDW. In addition, the water absorption of finer FDW particles may affect the internal structure formation of calcium-silicate-hydrate (C-S-H) of OPC. This phenomenon similarly occurred for SCC with 0.45-w/b as shown in Fig. 6 (b).

3.2 Properties of SCC in hardened state

3.2.1 Compressive and splitting tensile strengths

Fig. 7 shows the results of the averaging compressive strength test of SCC. Throughout the 180 days of testing, the compressive strength of the control SCC, SCC containing RHA, and RHA containing FDW continuously increased; the developing rate was high in the early stage and decreased after 90 days.

The SCC with RHA (without FDW) has a higher strength development after the final setting time than the control 0.35- and 0.45- w/b because untreated (unprocessed) RHA has a constant pozzolan reaction, which increases the compressive strength development. On

249 average, at 180 days of curing, the compressive strength of 10%wt RHA-SCC is 6.64 and
250 6.71% higher than 0.35-w/b and 0.45-w/b, respectively (Figs. 7 (a) and 7(b)). Moreover, when
251 FDW is added in the SCC with RHA, the compressive strength is 4.05 and 3.81% higher than
252 that of the control SCC and 10%wt RHA-SCC, respectively, because after the setting time,
253 some finer parts of FDW can fill and create a dense internal structure of SCC, particularly the
254 interfacial transition zone between OPC and river sand particles.
255 As shown in Figs. 7 and 8, the splitting tensile strength (**y**) and compressive strength (**x**)
256 increase and can be plotted with the w/b (Fig. 9) in Eqs. (1) - (2) as follows:
257
258 **y = 0.126x - 0.246**; R^2 = 0.9930 for w/b = 0.35 (1)
259 **y = 0.125x - 0.216**; R^2 = 0.9916 for w/b = 0.45 (2)
260
261 **4. Conclusions**
262 Based on the results of this investigation, the following conclusions are drawn:
263 • To achieve the targeted flow slump of SCC (70.0 ± 2.5 cm), the FDW replacement
264 of up to 50%wt increases the superplasticizer requirement more than the control
265 SCC and SCC mixed with RHA while decreasing the fresh density compared to the
266 control SCC.
267 • The use of FDW considerably increases the V-funnel flow time. The RHA-SCC
268 mixture containing FDW increases the flow time. In addition, SCC mixtures
269 prepared with 10 and 20%wt RHA have no noticeable blocking.
270 • Based on the workability requirements specified by EFNARC guidelines, SCC
271 mixtures exhibited acceptable V-funnel performance when they made RHA and
272 FDW at replacement levels of RHA and FDW not more than 10 and 30 wt%.

- SCC containing RHA and FDW has higher compressive and splitting tensile strengths than the control SCC. The 10% RHA-SCC with 30%wt FDW achieved the highest strength.
- It is possible to use RHA and FDW as materials in the production of economically friendly SCC. Not only can the replacement of OPC reduce CO_2 emissions by decreasing the OPC but the recycling of fine aggregate as partial replacement in river sand can also develop sustainability of SCC production.

Acknowledgements

This research has received funding from the European Union's Horizon 2020 Research and Innovation Programme under grant agreement no. 777823 and the Faculty of Industrial Technology at the Phranakhon Rajabhat University. The contributions of the PNRU laboratory staff are greatly appreciated.

References

[1] Md. Safiuddin, J.S. West, K.A. Soudki, Properties of freshly mixed self-consolidating concretes incorporating rice husk ash as a supplementary cementing material. Constr. Build. Mater. 30 (2012) 833–842.

[2] R.N. Kraus, T.R. Naik, B.W. Ramme, R. Kumar, Use of foundry silica-dust in manufacturing economical self-consolidating concrete. Constr. Build. Mater. 23 (2009) 3439–3442.

[3] N. Pathak, R. Siddique, Effects of elevated temperatures on properties of self-compacting-concrete containing fly ash and spent foundry sand. Constr. Build. Mater. 34 (2012) 512–521.

297 [4] G. Sua-Iam, N. Makul, Utilization of coal- and biomass-fired ash in the production of self-
298 consolidating concrete: a literature review. J. Clean. Prod. 100 (2015) 59–76.
299 [5] G. Sua-iam, P. Sokrai, N. Makul, Novel ternary blends of Type 1 Portland cement, residual
300 rice husk ash, and limestone powder to improve the properties of self-compacting concrete.
301 Constr. Build. Mater. 125 (2016) 1028–1034.
302 [6] M. Şahmaran, M.Lachemi, T.K.Erdem, H.E.Yücel, Use of spent foundry sand and fly ash
303 for the development of green self-consolidating concrete. Mater. Struct. 44 (2011) 1193–
304 1204.
305 [7] H.T. Le, H.-M.Ludwig, Effect of rice husk ash and other mineral admixtures on properties
306 of self-compacting high performance concrete. Mater. Design. 89 (2016) 156–166.
307 [8] E.M. Raisi, J.V. Amiri, M.R. Davoodi, Mechanical performance of self-compacting
308 concrete incorporating rice husk ash. Constr. Build. Mater. 177 (2018) 148–157.
309 [9] R.K. Sandhu, R. Siddique, Influence of rice husk ash (RHA) on the properties of self-
310 compacting concrete: A review. Constr. Build. Mater. 153 (2017) 751–764.
311 [10] S.N. Raman, T. Ngo, P. Mendis, Mahmud, H.B., High-strength rice husk ash concrete
312 incorporating quarry dust as a partial substitute for sand. Constr. Build. Mater. 25 (2011)
313 3123–3130.
314 [11] B.S. Thomas, Green concrete partially comprised of rice husk ash as a supplementary
315 binder material - A comprehensive review. Renew. Sust. Ener. Rev. 82 (2018) 3913–3923.
316 [12] H. Huang, X. Gao, H. Wang, H. Ye, Influence of rice husk ash on strength and
317 permeability of ultra-high performance concrete. Constr. Build. Mater. 149 (2017) 621–
318 628.
319 [13] P. Smarzewski, D. Barnat-Hunek, Mechanical and durability related properties of high
320 performance concrete made with coal cinder and waste foundry sand. Constr. Build. Mater.
321 121 (2016) 9–17.

322 [14] R. Siddique, G. Singh, Utilization of waste foundry sand (WFS) in concrete
323 manufacturing. Resour. Conserv. Recy. 55 (2011) 885–892.
324 [15] Y. Guney, Y.D. Sari, M. Yalcin, A. Tuncan, S. Donmez, Re-usage of waste foundry sand
325 in high-strength concrete. Waste Manag. 30 (2010) 1705–1713.
326 [16] R. Siddique, A. Noumowe, Utilization of spent foundry sand in controlled low-strength
327 materials and concrete. Resour. Conserv. Recy. 53 (2008) 27–35.
328 [17] B. Bhardwaj, P. Kumar, Waste foundry sand in concrete: A review. Constr. Build. Mater.
329 156 (2017) 661–674.
330 [18] N. Makul, G. Sua-Iam, Innovative utilization of foundry sand waste obtained from the
331 manufacture of automobile engine parts as a cement replacement material in concrete
332 production. J. Clean. Prod. 199 (2018) 305–320.
333 [19] N. Makul, P. Sokrai, Influences of fine waste foundry sand from the automobile engine-
334 part casting process and water-binder ratio on the properties of concrete: A new approach to
335 use of a partial cement replacement material. J. Build. Eng. 20 (2018) 544–558.
336 [20] R. Siddique, G. Singh, R. Belarbi, K. Ait-Mokhtar, Kunal, Comparative investigation on
337 the influence of spent foundry sand as partial replacement of fine aggregates on the
338 properties of two grades of concrete. Constr. Build. Mater. 83 (2015) 216–222.
339 [21] A. Torres, L. Bartlett, C. Pilgrim, Effect of foundry waste on the mechanical properties of
340 Portland cement concrete. Constr. Build. Mater. 135 (2017) 674–681.
341 [22] ASTM C150/C150M−12, Standard specification for Portland cement, ASTM
342 International, West Conshohocken, PA, 2012, 9 pp.
343 [23] ASTM C33/C33M−18, Standard specification for concrete aggregates, ASTM
344 International, West Conshohocken, PA, 2018, 8 pp.
345 [24] ASTM C494/C494−17, Standard specification for chemical admixtures for concrete,
346 ASTM International, West Conshohocken, PA, 2017, 10 pp.

[25] ASTM C1611/C1611M−14, Standard test method for slump flow of self-consolidating concrete, ASTM International, West Conshohocken, PA, 2011, 6 pp.
[26] ASTM C1621/C1621M−17, Standard test method for passing ability of self-consolidating concrete by J-Ring, ASTM International, West Conshohocken, PA, 2011, 11 pp.
[27] EFNARC, Specification and guidelines for self-compacting concrete, European Federation of Producers and Applicators of Specialist Products for Structures, 2002, 32 pp.
[28] ASTM C138/C138M−17a, Standard test method for density (unit weight), yield, and air content (gravimetric) of concrete, ASTM International, West Conshohocken, PA, 2017, 6 pp.
[29] ASTM C403/C403M−16, Standard test method for time of setting of concrete mixtures by penetration resistance, ASTM International, West Conshohocken, PA, 2017, 7 pp.
[30] ASTM C39/C39M−18, Standard test method for compressive strength of cylindrical concrete specimens, ASTM International, West Conshohocken, PA, 2017, 8 pp.
[31] ASTM C496/C496M−17, Standard test method for splitting tensile strength of cylindrical concrete specimens, ASTM International, West Conshohocken, PA, 2017, 5 pp.

Figure captions

Fig. 1 Particle size distributions of OPC, FDW, and RHA in the semilogarithmic scale.

Fig. 2 SEM micrographs (5000×) of (a) OPC, (b) RHA, and (c) FDW.

Fig. 3 Required superplasticizer of the SCC mixtures.

Fig. 4 V-funnel flow time of the SCC mixtures.

Fig. 5 Slump flow loss at 120 min for the SCC mixtures.

Fig. 6 Setting times of the SCC mixtures.

Fig. 7 Compressive strengths of concrete prepared with (a) w/b = 0.35 and (b) w/b = 0.45 and a binder material content of 650 kg/m^3.

Fig. 8 Splitting tensile strengths of concrete prepared with (a) w/b = 0.35 and (b) w/b = 0.45 and a binder material content of 650 kg/m^3.

Fig. 9 Relationship between the compressive strength and splitting tensile strength and the (a) binder material content and (b) w/b ratios of the SCC mixture.

Table 1 Mixture proportions of SCC.

SCC Type	w/b ratio	Powder materials (kg/m^3)	OPC (kg/m^3)	RHA (kg/m^3)	Sand (kg/m^3)	FDW (kg/m^3)	Crushed limestone rock (kg/m^3)	Water (kg/m^3)
65R0FDW0	0.35	650	650	0	961	0	828	227.5
65R10FDW0	0.35	650	585	65	961	0	828	227.5
65R20FDW0	0.35	650	520	130	961	0	828	227.5
65R10FDW30	0.35	650	585	65	673	288	828	227.5
65R10FDW50	0.35	650	585	65	481	481	828	227.5
65R20FDW30	0.35	650	520	130	673	288	828	227.5
65R20FDW50	0.35	650	520	130	481	481	828	227.5
65R0FDW0	0.45	650	650	0	961	0	828	292.5
65R10FDW0	0.45	650	585	65	961	0	828	292.5
65R20FDW0	0.45	650	520	130	961	0	828	292.5
65R10FDW30	0.45	650	585	65	673	288	828	292.5
65R10FDW50	0.45	650	585	65	481	481	828	292.5
65R20FDW30	0.45	650	520	130	673	288	828	292.5
65R20FDW50	0.45	650	520	130	481	481	828	292.5

Remarks: [1] **XRYUZ** denotes the following: **X** is the powder material content (OPC + RHA) (650 kg/m^3), **RY** is the percentage OPC replacement of the rice husk ash (RHA) content (0%, 10%, and 20% wt.), and **FDWZ** is the percentage sand replacement of the foundry sand (FS) content (0%, 30%, and 50% wt.).

Table 2 Chemical composition and physical properties of OPC, RHA, and FDW.

Chemical composition (Percentage by mass, %)	OPC (Mean + SD)	RHA (Mean + SD)	FDW (Mean + SD)
SiO_2	19.84 ± 0.52	91.45 ± 1.34	82.19 ± 1.24
Al_2O_3	4.21 ± 0.28	0.44 ± 0.06	4.76 ± 0.31
Fe_2O_3	3.19 ± 0.09	0.18 ± 0.02	2.63 ± 0.28
MgO	1.25 ± 0.02	0.36 ± 0.20	0.77 ± 0.08
CaO	68.02 ± 1.06	0.99 ± 0.07	1.34 ± 0.42
Na_2O	0.18 ± 0.03	0.11 ± 0.02	0.75 ± 0.04
K_2O	0.33 ± 0.06	1.39 ± 0.03	0.59 ± 0.09
SO_3	3.57 ± 0.19	0.14 ± 0.02	0.22 ± 0.04
Loss on ignition	0.92 ± 0.04	1.39 ± 0.03	3.63 ± 0.19
Particle size at 50% cumulative passing (μm)	13.50 ± 0.39	22.31 ± 0.88	23.85 ± 0.42
Specific gravity	3.14 ± 0.02	2.32 ± 0.05	2.42 ± 0.01
Specific surface area (m^2/kg) BET-method	382 ± 5.02	364 ± 9.04	341 ± 8.25

Table 3 Fresh state properties of the SCC mixtures.

Mixture labels	w/b ratio	Targeted flow slump (cm)	J-ring test (initial) (cm)	Difference (initial) (cm)	Blocking assessment[1]	V-funnel flow time (s)	Fresh density	
							value (kg/m^3)	% control
65R0FDW0	0.35	72	70	2	No visible blocking	7	2,454	100
65R10FDW0	0.35	72	70	2	No visible blocking	9	2,439	-0.60
65R20FDW0	0.35	72	60	10	No visible blocking	10	2,424	-1.24
65R10FDW30	0.35	71	68	3	Noticeable blocking	12	2,425	-1.20
65R10FDW50	0.35	72	68	4	Noticeable blocking	14	2,415	-1.60
65R20FDW30	0.35	71	66	5	Noticeable blocking	16	2,410	-1.80
65R20FDW50	0.35	70	65	5	Noticeable blocking	20	2,400	-2.20
65R0FDW0	0.45	72	71	1	No visible blocking	6	2,402	-2.12
65R10FDW0	0.45	71	70	1	No visible blocking	7	2,386	-2.76
65R20FDW0	0.45	70	69	1	No visible blocking	8	2,372	-3.36
65R10FDW30	0.45	72	70	2	No visible blocking	9	2,373	-3.32
65R10FDW50	0.45	72	69	3	Noticeable blocking	10	2,363	-3.72
65R20FDW30	0.45	71	67	4	Noticeable blocking	13	2,357	-3.96
65R20FDW50	0.45	71	66	5	Noticeable blocking	14	2,348	-4.32

Remark: [1] For the blocking assessment, the differences in slump flow and J-ring flow diameters were determined. In this assessment, 0–2.5 cm is defined as no visible blocking, 2.5–5.0 cm) is defined as minimal to noticeable blocking, and greater than 5.0 cm is defined as noticeable to extreme blocking.

Figures

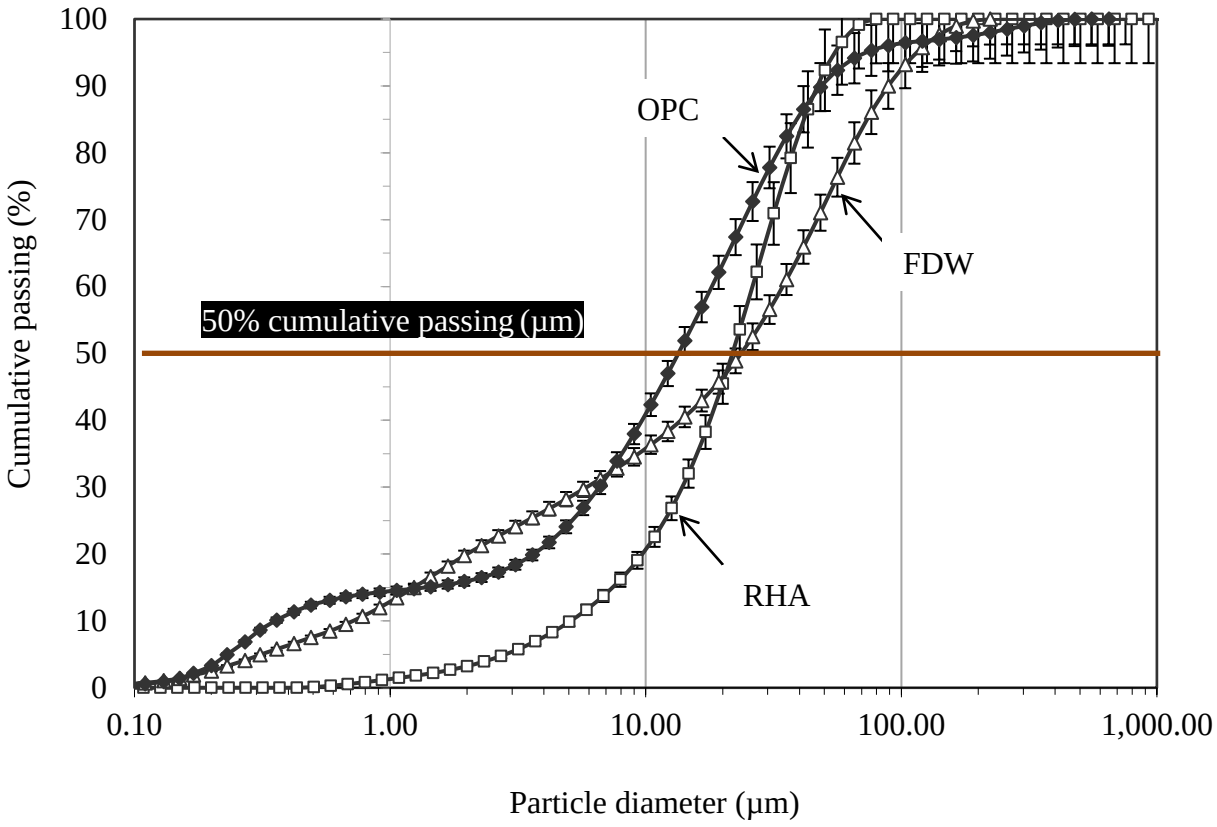

Fig. 1 Particle size distributions of OPC, FDW, and RHA in the semilogarithmic scale.

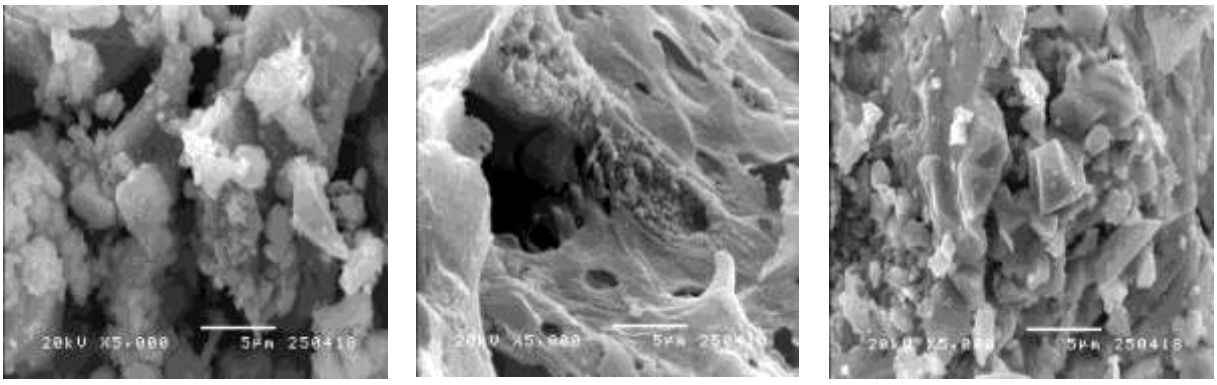

(a) (b) (c)

Fig. 2 SEM micrographs (5000×) of (a) OPC, (b) RHA, and (c) FDW.

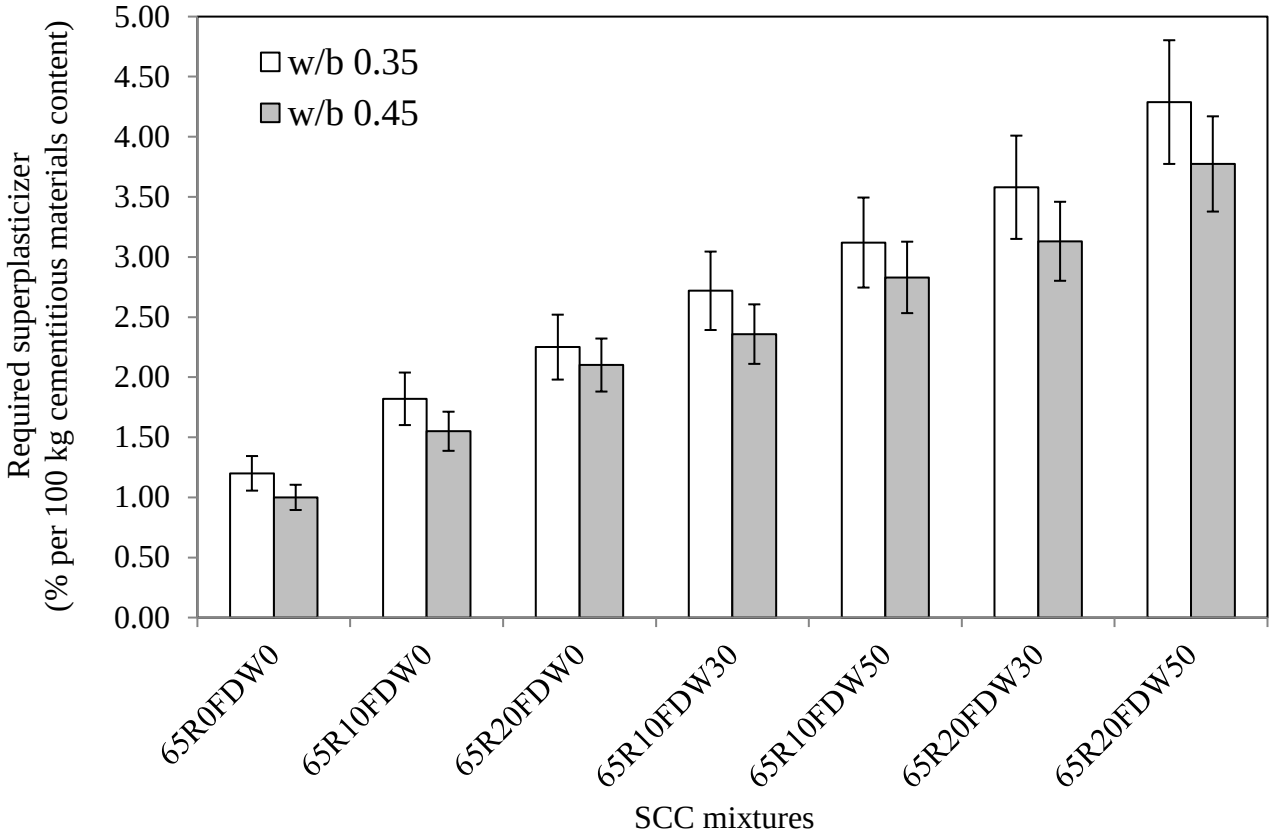

Fig. 3 Required superplasticizer of the SCC mixtures.

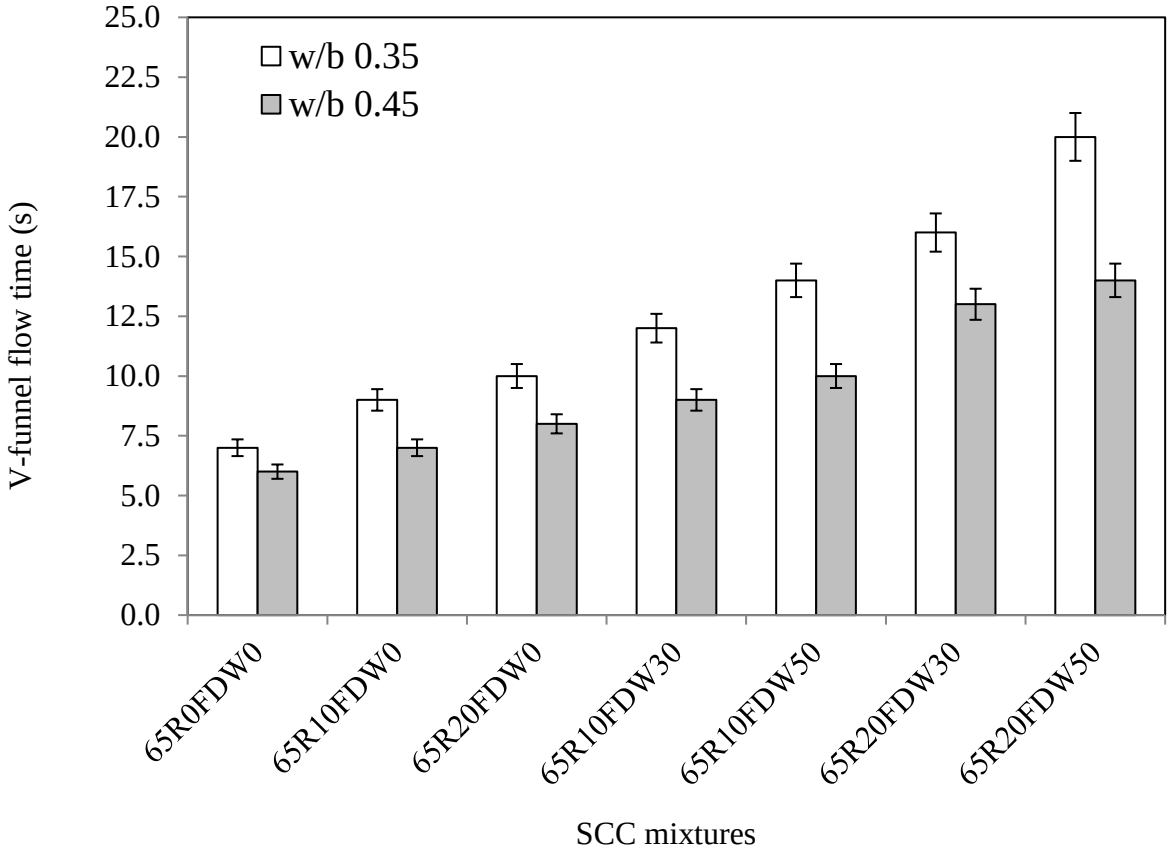

Fig. 4 V-funnel flow time of the SCC mixtures.

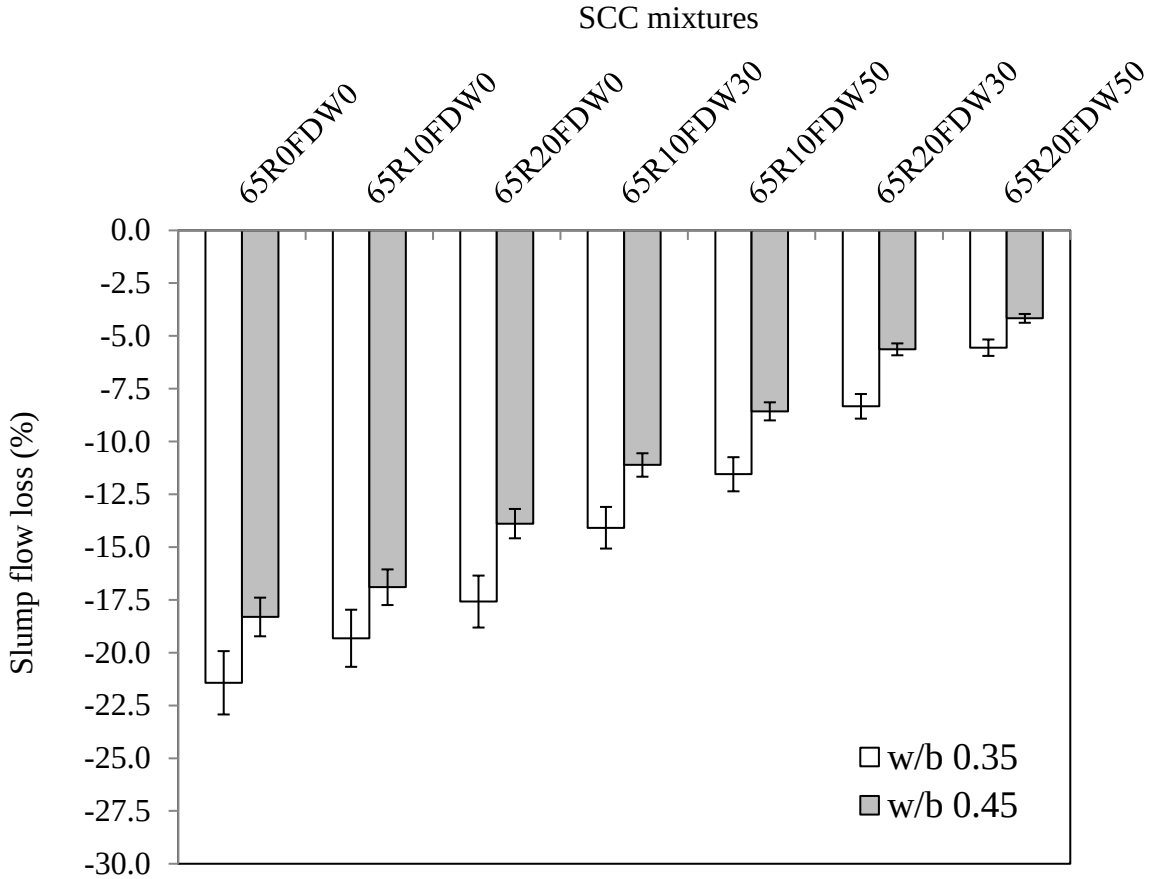

Fig. 5 Slump flow loss at 120 min for the SCC mixtures.

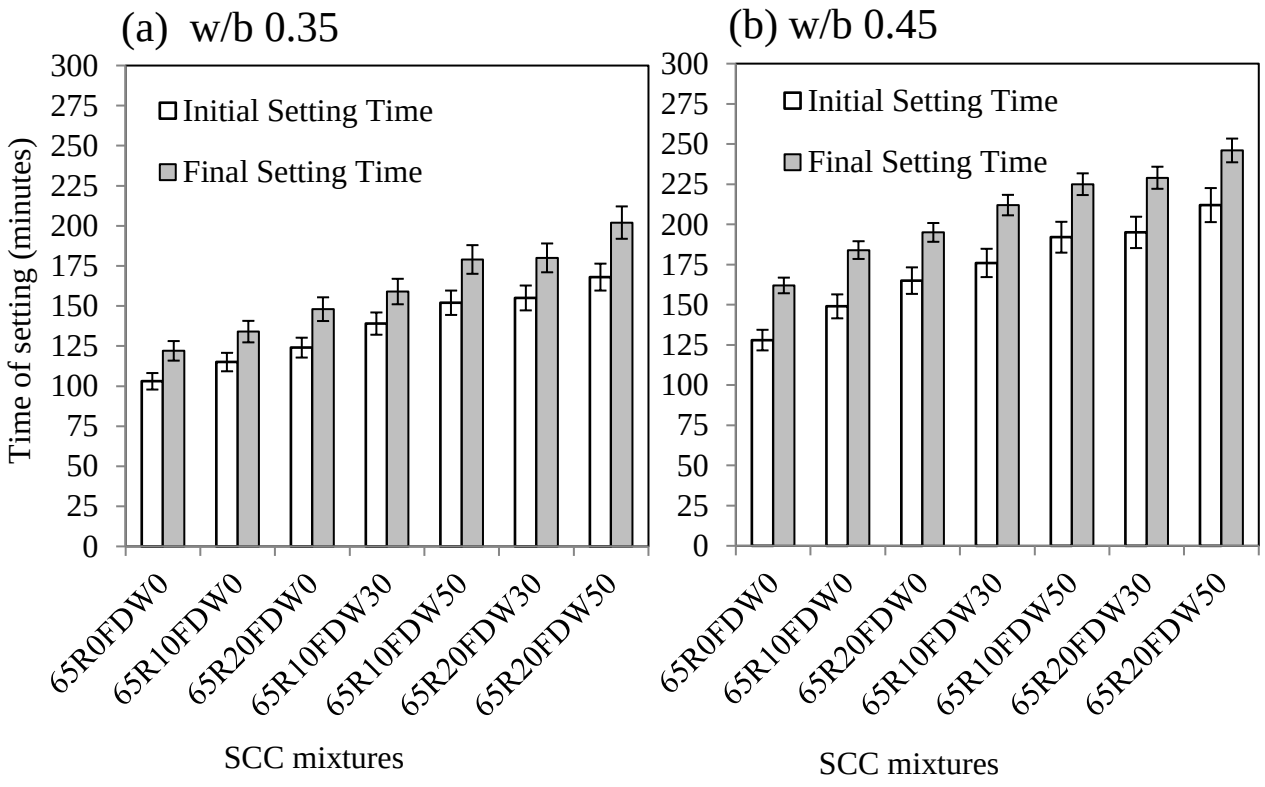

Fig. 6 Setting times of the SCC mixtures.

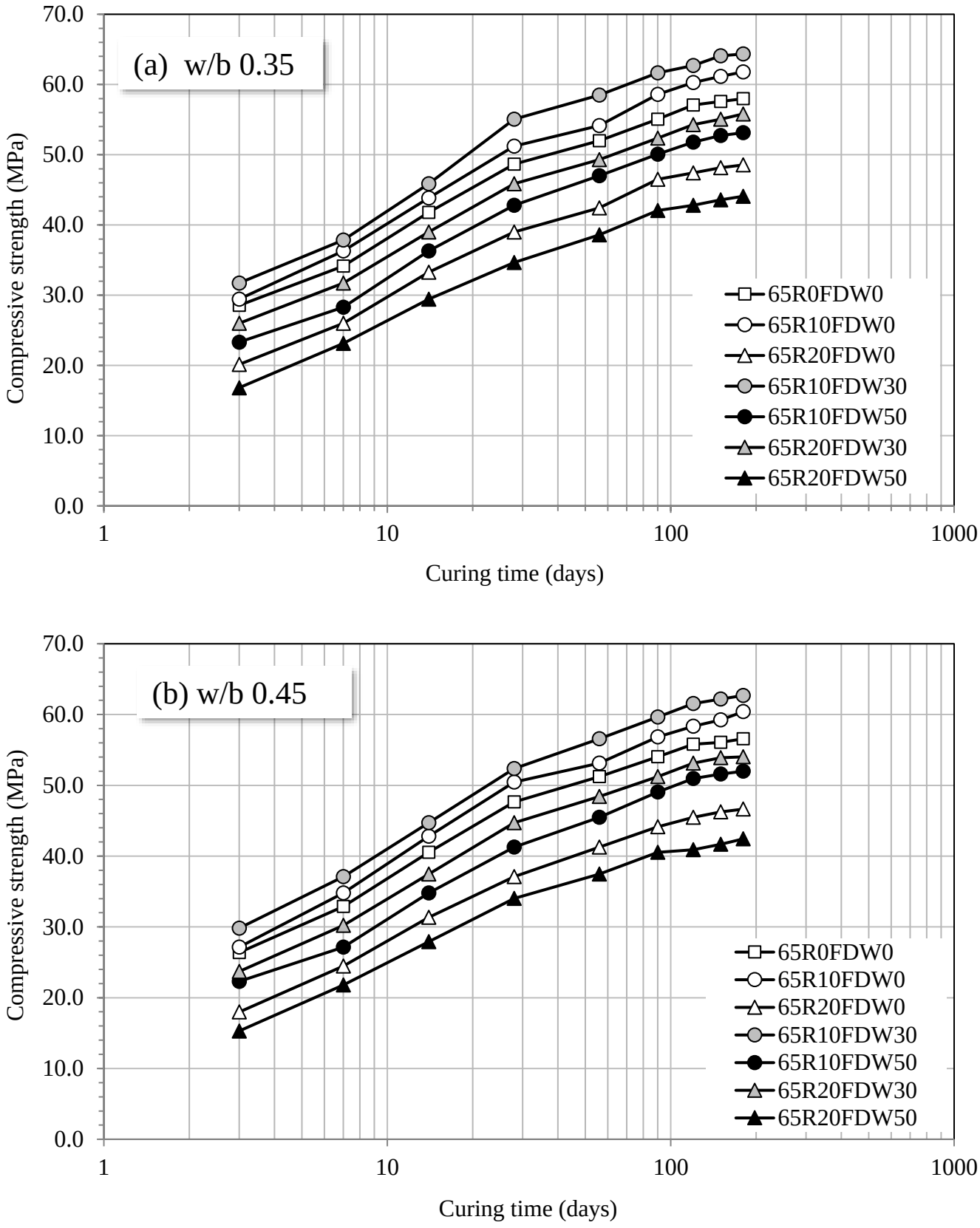

Fig. 7 Compressive strengths of concrete prepared with (a) w/b = 0.35 and (b) w/b = 0.45 and a binder material content of 650 kg/m^3.

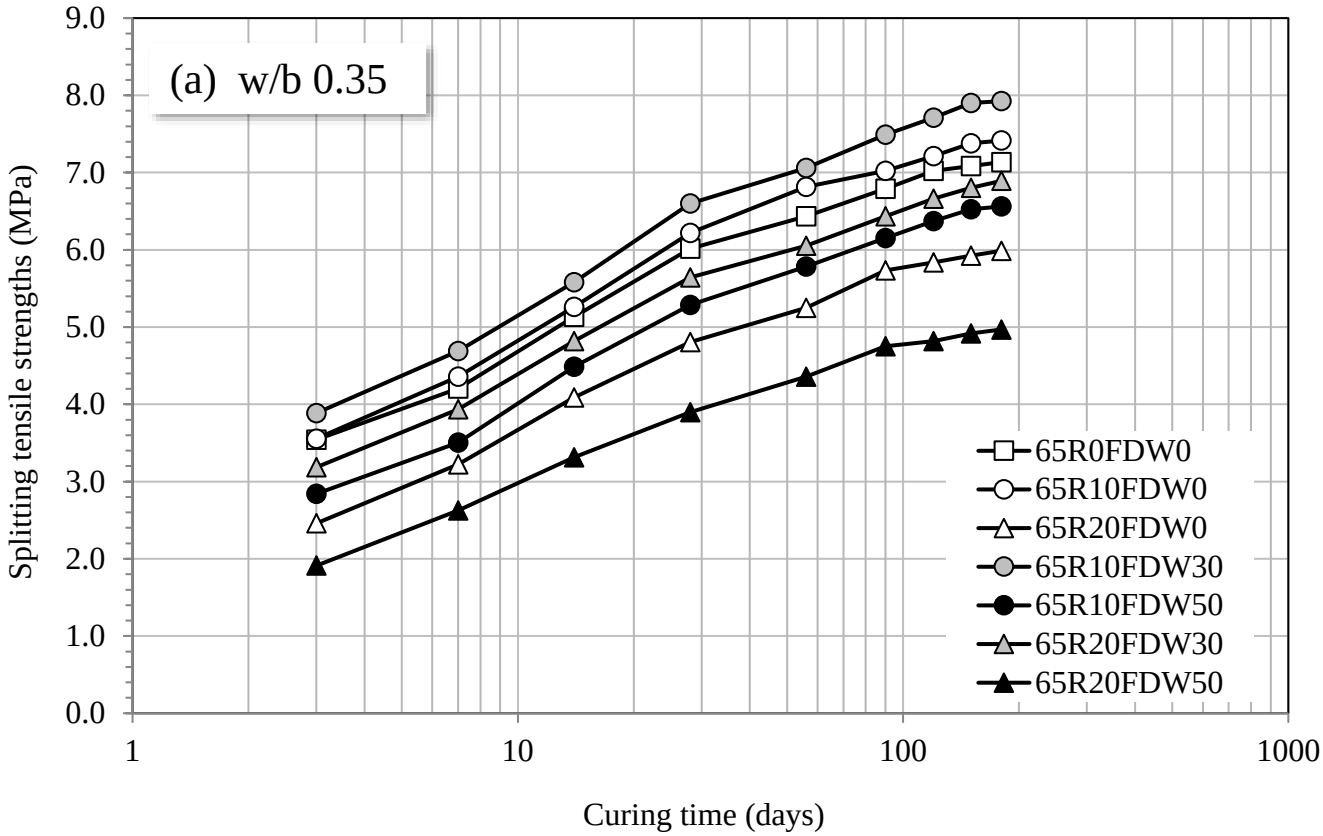

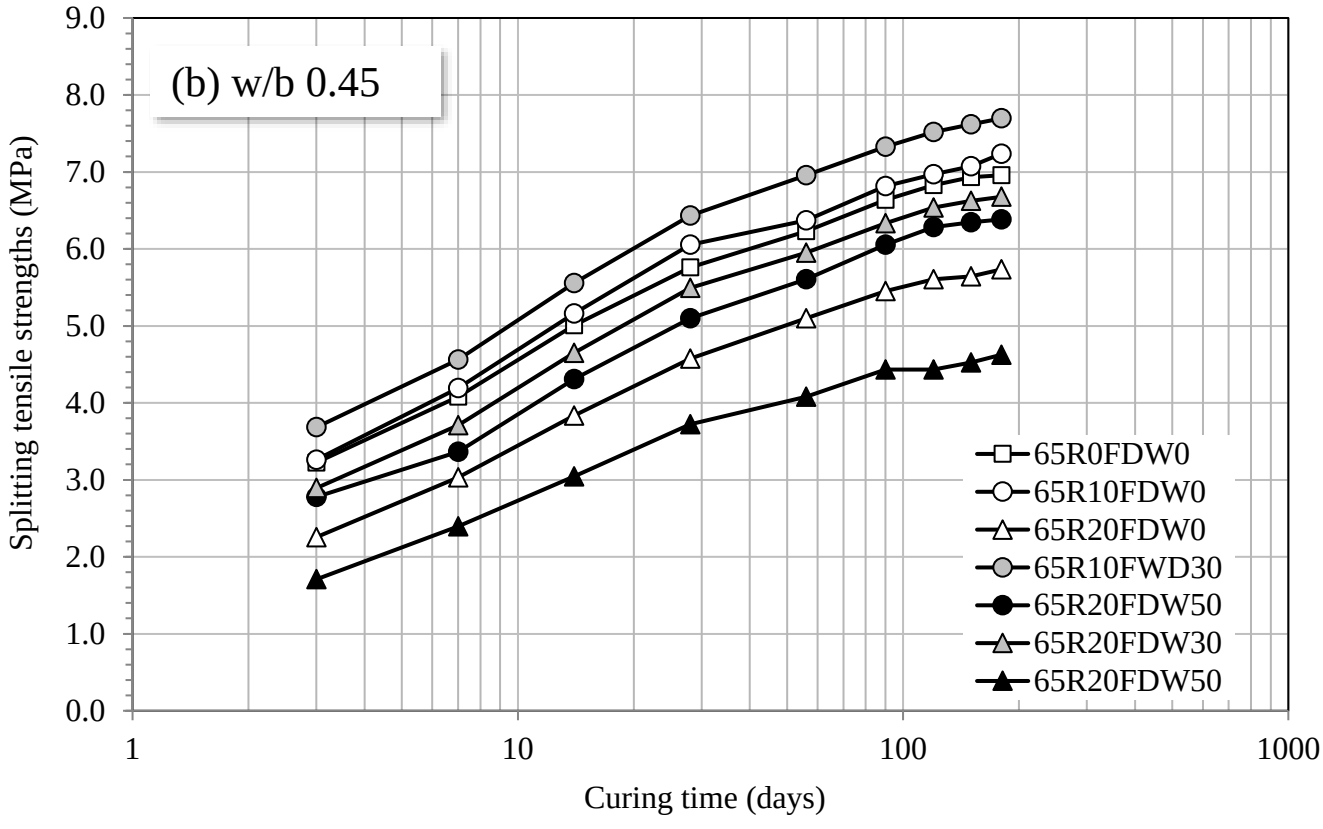

Fig. 8 Splitting tensile strengths of concrete prepared with (a) w/b = 0.35 and (b) w/b = 0.45 and a binder material content of 650 kg/m^3.

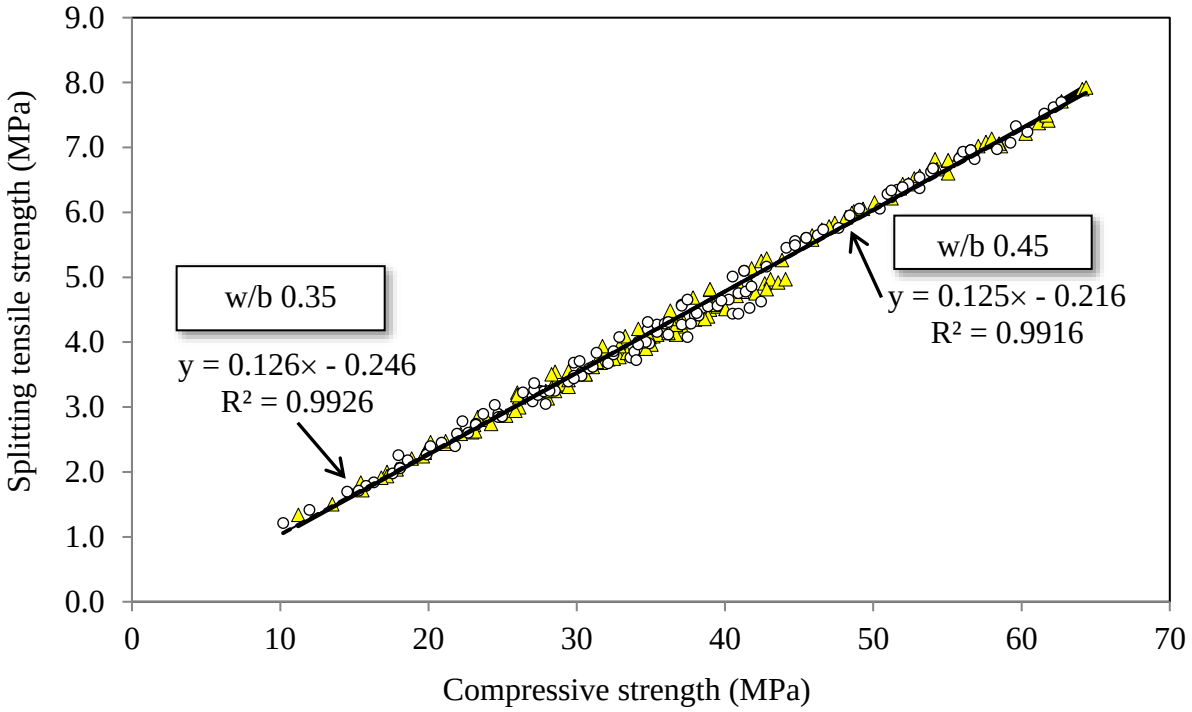

Fig. 9 Relationship between the compressive strength and splitting tensile strength and the w/b of the SCC mixture.